INSTITUTE OF PHYSICS PUBLISHING MEASUREMENT SCIENCE AND TECHNOLOGY
Meas. Sci. Technol. **13** (2002) 533–538 PII: S0957-0233(02)30971-8

Electrical current metering with a dual interferometric configuration and serrodyne signal processing

P A S Jorge[1,2], P Caldas[1,2], L A Ferreira[3], A B Lobo Ribeiro[3], J L Santos[1,2] and F Farahi[4]

[1] Unidade de Optoelectrónica e Sistemas Electrónicos, INESC-Porto, Rua do Campo Alegre, 687, 4169 007 Porto, Portugal
[2] Departamento de Física da Faculdade de Ciências da Universidade do Porto, Rua do Campo Alegre, 687, 4169 007 Porto, Portugal
[3] MultiWave Networks Portugal, Lda., R. Eng. Frederico Ulrich, 2650, 4470-605 Moreira da Maia, Portugal
[4] Physics Department, University of North Carolina at Charlotte, Charlotte, NC 28223, USA

E-mail: pjorge@inescporto.pt

Received 20 November 2001, accepted for publication 29 January 2002
Published 28 February 2002
Online at stacks.iop.org/MST/13/533

Abstract
A bulk interferometric configuration for electrical current remote sensing in high voltage environments based on the Faraday effect is described. The combination of Sagnac's reciprocal properties with a Mach–Zehnder processing interferometer in the same sensing head is used to implement serrodyne processing for current sensing. A theoretical analysis based on the Jones matrix is presented. Experimental results that validate the exploited concept are obtained, showing linearity up to 1800 A_{rms} and waveform reproduction at 50 Hz. The possibility of using the proposed interferometric concept to simultaneously fulfil the requirements associated with metering and relaying applications is also addressed.

Keywords: optical current sensors, Faraday effect, interferometric demodulation

1. Introduction

Optical technology for the measurement of electrical current in high voltage environments has experienced considerable development in the last decade [1, 2]. Due to the intrinsic dielectric characteristics of optical sensors the need for insulation is greatly reduced. The optical phenomenon on which most configurations are based, the Faraday effect, has a constant linear response over a wide range of frequencies and, unlike conventional sensors, presents no hysteresis or saturation effects for realizable fields. Bulk closed loop configurations, illuminated remotely by optical fibre guided radiation, are especially attractive because their closed optical path ensures immunity to external magnetic fields, allowing therefore univocal current measurement. Also, bulk materials with a high Verdet constant and a small stress-optical coefficient can be chosen that minimize the linear birefringence problems common to all-fibre configurations [3]. Several closed bulk optical circuit solutions have been presented. Among the most successful are a triangular critical angle reflection sensing head [4], a square shaped sensing head with double complementary reflections in the corners [5] and a multiple critical angle reflection ring shaped sensing head [6].

The Faraday effect consists of a circular birefringence induced in the medium by the presence of a magnetic field. This causes a linear polarized state to rotate its plane of vibration by an angle θ_F given by

$$\theta_F = \int_L V \vec{\boldsymbol{H}} \cdot \mathrm{d}\vec{l} \tag{1}$$

where V is the material-dependent Verdet constant, $\vec{\boldsymbol{H}}$ is the magnetic field and L is the interaction length. In most bulk configurations the polarization azimuth current dependence is converted into an optical power modulation with a polarimetric scheme. Typically the detected irradiance

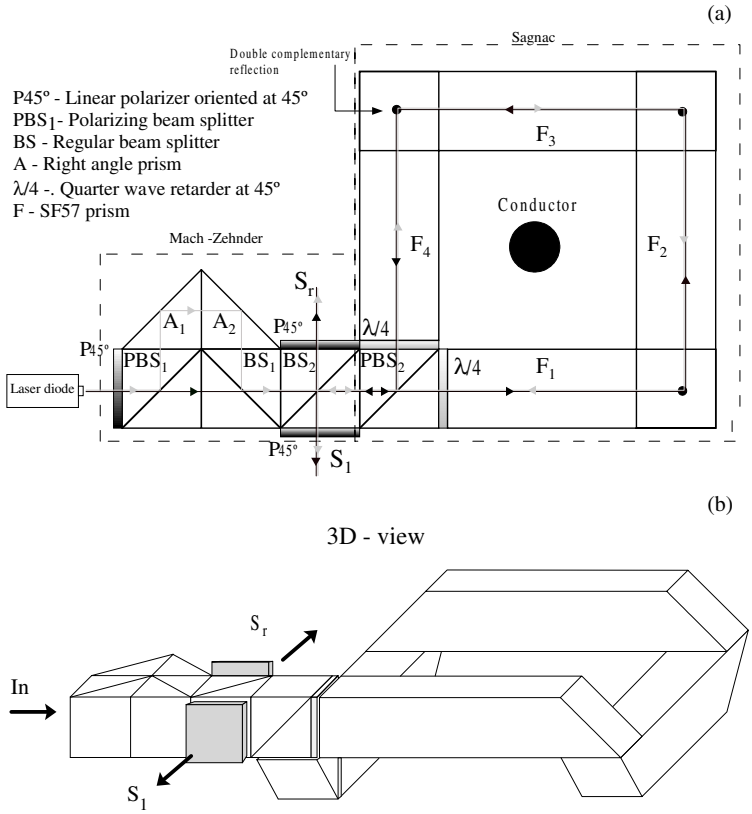

Figure 1. (*a*) Schematic representation of the proposed configuration; (*b*) 3D view.

exhibits a sinusoidal dependence with the azimuth angle. This means that the working range must be restricted to the linear part of the transfer function, or some kind of feedback must be used in order to linearize the output. Also, the optical power fluctuations due to vibrations or optical source instability must be compensated by some reference scheme in order to recover the measurement information without ambiguity [7].

The scheme introduced here is a bulk interferometric configuration where the measurement information appears as a phase modulation of a high frequency carrier. In this way the sensor transfer function is independent of optical power fluctuations and has a truly linear dependence with the current.

2. Principle of operation

The proposed sensing head, represented schematically in figure 1, is a Mach–Zehnder processing interferometer with an additional reciprocal loop. The square shaped loop, which consists of a Sagnac interferometer, is built with low linear birefringence SF57 glass prisms. In order for the beam to remain confined within this loop internal reflections are needed at the corners. To avoid unwanted phase terms the technique of double reflections with complementary effects in each corner was used [5].

Linear polarized light entering the first interferometer is split by PBS_1 into two orthogonal linear modes that follow different paths. These modes are recombined in the Mach–Zehnder outputs. When viewed through a linear polarizer oriented at 45°, an interferometric reference signal is obtained in one of the BS_2 outputs (S_r). The optical path imbalance between the two beams allows a high frequency carrier to be generated by ramping the laser diode injection current. The optical radiation that is not reflected towards the polarizer at the third beam splitter (BS_2) illuminates the square loop. At this point the orthogonal linear modes are converted, by the $\lambda/4$ retardation plates oriented at 45°, into two counter-propagating orthogonal circular polarized modes. After circling the loop the two circular modes, passing once again through the retardation plates, are reconverted into linear orthogonal modes. This radiation is reflected in BS_2 and, after crossing a linear polarizer at 45°, originates an interferometric output signal (S_1). Due to the circular birefringence induced in the square loop by the magnetic field, a phase difference is introduced between the two orthogonal circular modes which is proportional to the current under measurement. This way the pseudo-heterodyne carrier generated in the first interferometer is phase modulated by the measuring current in the second interferometer.

This configuration has several advantages for use in optical current measurements. The measurement information, which is contained in the carrier phase, is not corrupted by optical power fluctuations. Furthermore, the Sagnac topology is intrinsically insensitive to reciprocal effects like those induced by vibrations or temperature fluctuations and responds only to non-reciprocal effects like the Faraday effect [8]. Also, the use of serrodyne demodulation avoids low frequency electronic noise. The phase information in output S_1 is extracted with a lock-in amplifier using output S_r as a reference signal. This provides some degree of immunity to the optical source spectral instability and the correspondent phase noise.

3. Theory and simulation results

The proposed system can be mathematically modelled using Jones matrix notation [9]. For simplicity ideal conditions are considered: the current under measurement is assumed to be passing through the centre of the sensing head in a direction which is perpendicular to the sensor plane; there are no external fields present near the sensor; all reflections in the corners occur exactly at the same angle (45°); and, finally, the sensing prisms are considered free from any linear birefringence. Under these conditions the effects of reflections and propagation in the corners can be ignored, and the square sensing module can be treated as a single prism with a quarter of the total interaction length and fourfold sensitivity.

The electrical field vectors ($\vec{E}_1$ and $\vec{E}_2$) associated with each of the orthogonal linear modes in the reference output are given by

$$\vec{E}_1 = P[45^\circ] \cdot \mathrm{BS}_2 \cdot \mathrm{BS}_1 \cdot \mathrm{PBS}_1[90^\circ] \cdot \vec{E}_i \tag{2}$$

and

$$\vec{E}_2 = P[45^\circ] \cdot \mathrm{BS}_2 \cdot \mathrm{BS}_1 \cdot \mathrm{PBS}_1[0^\circ] \cdot \vec{E}_i \, \mathrm{e}^{-\mathrm{i}\Delta\phi}. \tag{3}$$

In both equations the initial field $\vec{E}_i$ is considered after crossing the input polarizer oriented at 45° and is given by

$$\vec{E}_i = \frac{E_0}{\sqrt{2}} \begin{pmatrix} 1 \\ 1 \end{pmatrix} \tag{4}$$

where E_0 corresponds to the electrical field amplitude of the assumed depolarized radiation before the polarizer. In equations (2) and (3), $P[45^\circ]$, BS and $\mathrm{PBS}_1[90^\circ]$ represent the matrices corresponding to a linear polarizer oriented at 45°, a beam splitter and a polarizing beam splitter, respectively. The term $\Delta\phi$ represents the relative phase introduced by the Mach–Zehnder path imbalance and is given by

$$\Delta\phi = \frac{2\pi n \Delta l}{\lambda} \tag{5}$$

where n is the medium refractive index, λ is the radiation wavelength and Δl is the geometrical path imbalance of the interferometer. With the expressions obtained for the electrical field vectors the irradiance at output S_r can be derived as

$$S_r = (\vec{E}_1 + \vec{E}_2) \cdot (\vec{E}_1 + \vec{E}_2)^* \tag{6}$$

and

$$S_r = \frac{E_0^2}{8}(1 + \cos[\Delta\phi]). \tag{7}$$

On the other hand, the electrical field vectors originated by the two orthogonal linear modes at output S_1 ($\vec{E}_1'$ and $\vec{E}_2'$) can be calculated by the matrix expressions:

$$\begin{aligned}\vec{E}_1' = {} & P[45^\circ] \cdot \mathrm{BS}_2 \cdot \mathrm{PBS}_2[90^\circ] \cdot \lambda[4, -45^\circ] \cdot F[\theta_F] \\ & \cdot \lambda[4, 45^\circ] \cdot \mathrm{PBS}_2[90^\circ] \cdot \mathrm{BS}_2 \cdot \mathrm{BS}_1 \\ & \cdot \mathrm{PBS}_1[90^\circ] \cdot \vec{E}_i\end{aligned} \tag{8}$$

and

$$\begin{aligned}\vec{E}_2' = {} & P[45^\circ] \cdot \mathrm{BS}_2 \cdot \mathrm{PBS}_2[0^\circ] \cdot \lambda[4, -45^\circ] \cdot F[-\theta_F] \\ & \cdot \lambda[4, 45^\circ] \cdot \mathrm{PBS}_2[0^\circ] \cdot \mathrm{BS}_2 \cdot \mathrm{BS}_1 \\ & \cdot \mathrm{PBS}_1[0^\circ] \cdot \vec{E}_i \, \mathrm{e}^{-\mathrm{i}\Delta\phi}\end{aligned} \tag{9}$$

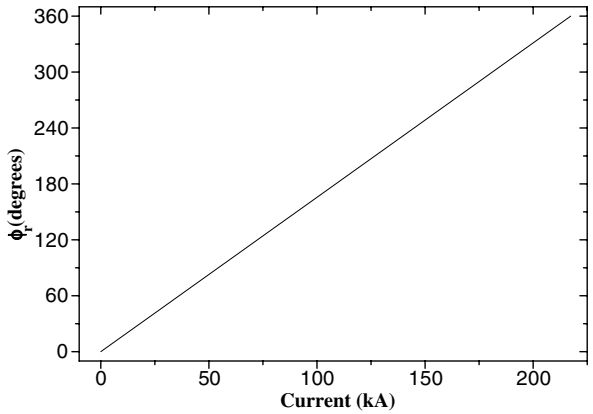

Figure 2. Sensor transfer function: relative phase versus applied current.

where $F[\theta_F]$ represents the effect of the magneto-optic medium. In the absence of linear birefringence this corresponds to a pure rotation matrix, where the rotation angle is given by the Faraday modulation. The matrix $\lambda[4, 45^\circ]$ stands for the quarter-wave retardation plates oriented at 45°. Calculating the irradiance at output S_1 it comes out as

$$S_1 = \frac{E_0^2}{16}(1 + \cos[\Delta\phi + 2\theta L]) \tag{10}$$

where θ is the Faraday rotation per unit length and L is the total interaction length.

When the injection current of the laser diode is modulated at a frequency ω and with amplitude required to sweep the interferometer over a phase of 2π, outputs S_1 and S_r would be functions of time:

$$S_r = \frac{E_0^2}{8}(1 + \cos[\omega t + \phi_0]) \tag{11}$$

and

$$S_1 = \frac{E_0^2}{16}(1 + \cos[\omega t + 2\theta L + \phi_0]). \tag{12}$$

Equations (11) and (12) were derived by ignoring the effect of fly-back distortion on the signals since this could easily be achieved via band-pass filtering. In these equations the term ωt results from the time variation imposed on the phase by the laser wavelength modulation and ϕ_0 is the quasi-static phase of the Mach–Zehnder interferometer that also includes the effect of environmental perturbations and the impact of instability in the laser's wavelength. Two carrier signals are therefore obtained: a reference signal with a quasi-static phase and an output signal with its phase modulated by the current being measured. Introducing these two signals into a lock-in amplifier, their relative phase can be obtained:

$$\phi_r = 2\theta L + \phi_0 - \phi_0 = 2\theta L. \tag{13}$$

This phase information can be related to the current passing through the conductor using equation (1) to calculate θ:

$$\theta = 2\frac{V}{L}\frac{\mu_0 I}{2\pi}\arctan\left[\frac{L}{2r}\right] \tag{14}$$

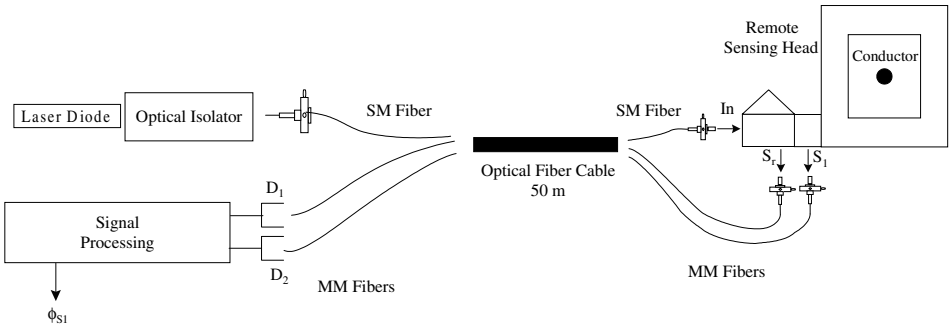

Figure 3. Experimental set-up implemented to test the proposed configuration.

where I is the electrical current, r is the distance between each prism and the conductor and μ_0 is the magnetic permeability of the medium (assumed non-magnetic).

With these expressions it becomes possible to predict the behaviour of the sensor transfer function. The system parameters are: $\lambda = 850$ nm; $V_{(\mathrm{SF57glass})} \approx 11.7$ rad m^{-1} T^{-1}; $r \approx 5$ cm; $L \approx 38$ cm (each side of the square loop is 9 cm). Figure 2 shows the theoretical dependence of the phase ϕ_r for a current excursion from zero to 217 kA. A perfectly linear phase response can be observed under ideal conditions. The corresponding phase excursion is approximately 360°, which results in a sensitivity of 1.7 ° kA^{-1}. This is a modest value, but this type of sensor is typically used to measure large electrical currents. On the other hand, the specific performance in terms of current resolution will, as always, be dependent on the minimization of the several noise sources present in the measurement system.

4. Experimental results

The experimental set-up used to demonstrate the feasibility of the proposed current sensor design is shown in figure 3.

A single-mode laser diode (Hitachi-HL8311E) operating at 830 nm with 7 mW of output power was used. To avoid back reflections into the laser cavity the input optical fibre end was cut at an angle and an optical isolator was placed between the collimating and injection lenses. The sensing head was connected to the optical source and the detection and processing electronics through a 50 m optical fibre cable. A single-mode fibre carries optical power to the sensing head and two multimode fibres carry the output signals to the detector.

To obtain good fringe visibility both arms in the Mach–Zehnder interferometer must receive similar levels of optical power. This was achieved by introducing a linear polarizer at 45° relative to the input polarizing beam splitter (PBS_1). The laser output polarization state was then carefully monitored and controlled in order to avoid any power fluctuations. In a practical situation, however, to improve the sensor performance the input radiation must be either completely depolarized or guided by an input PM fibre.

A low voltage current source providing outputs from 0 to 2000 A_{rms} and operating at 50 Hz was used to generate the current to be measured. The laser injection current was modulated at 2 kHz with a sawtooth waveform and the amplitude of the signal was adjusted to ≈1.6 mA in order to obtain a 2π phase modulation in the Mach–Zehnder

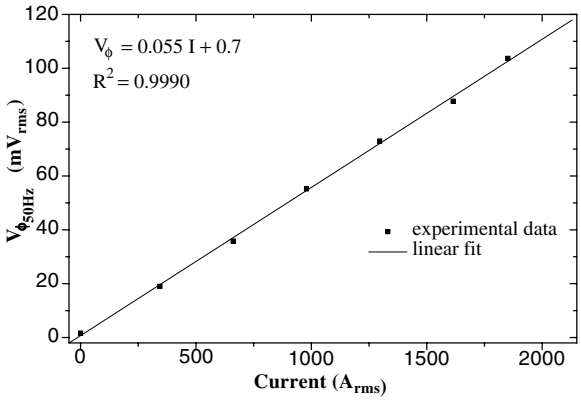

Figure 4. Experimental data showing system response to applied current.

interferometer (which had an optical path imbalance of ≈6 cm). The phase of carrier S_1 relative to the reference signal S_r was measured using a lock-in amplifier. The lock-in output was then fed into an electrical spectrum analyser, where an electrical signal proportional to the phase at 50 Hz ($V_{\phi_{50\ \mathrm{Hz}}}$, 1 V corresponds to 18°) was monitored.

Results relative to a linearity test (phase amplitude at 50 Hz versus applied current) are given in figure 4. From this figure, a good correlation between experimental data and linear fit can be observed, and a system sensitivity of 1° kA^{-1} (RMS) can be estimated. This result is in fair agreement with the theoretical predictions of 1.7 ° kA^{-1}, considering various assumptions were made to create a simple theoretical model.

The system functionality was tested by comparing the measured signal with the original current waveform that goes through the conductor. In order to obtain the current waveform a coil was incorporated in the vicinity of the conductor that introduces a $\pi/2$ phase shift in the induced signal. In figure 5, the upper traces are the measured signals and the lower traces are the current waveform with values of 1613 A_{rms} and 819 A_{rms}. It must be pointed out that the measured waveforms (upper traces) have been filtered, as the lock-in bandwidth was set to a value slightly higher than 50 Hz. The important point to retain here is that the behaviour of the sensor is identical for two different RMS values of current.

System resolution can be calculated by measuring the signal to noise ratio directly from the electrical spectrum. Figures 6(*a*) and (*b*) show the spectra of the electrical carrier and the recovered phase waveform, respectively, when a current of 100 A_{rms} was passing through the conductor.

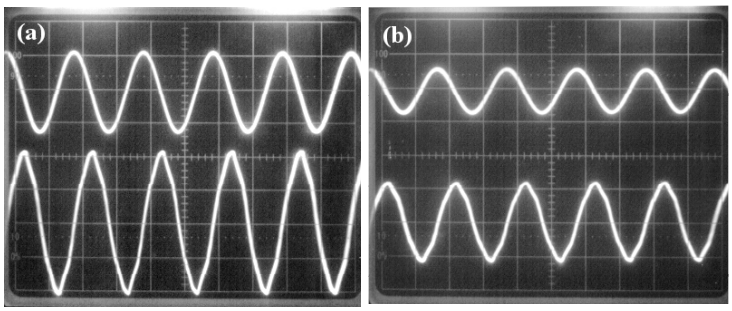

Figure 5. Evaluation of waveform reproduction. Signal proportional to the applied current phase shifted by $\pi/2$ (lower trace) and measured waveform (upper trace) for a current passing through the conductor with (*a*) 1613 A_{rms}; (*b*) 819 A_{rms}.

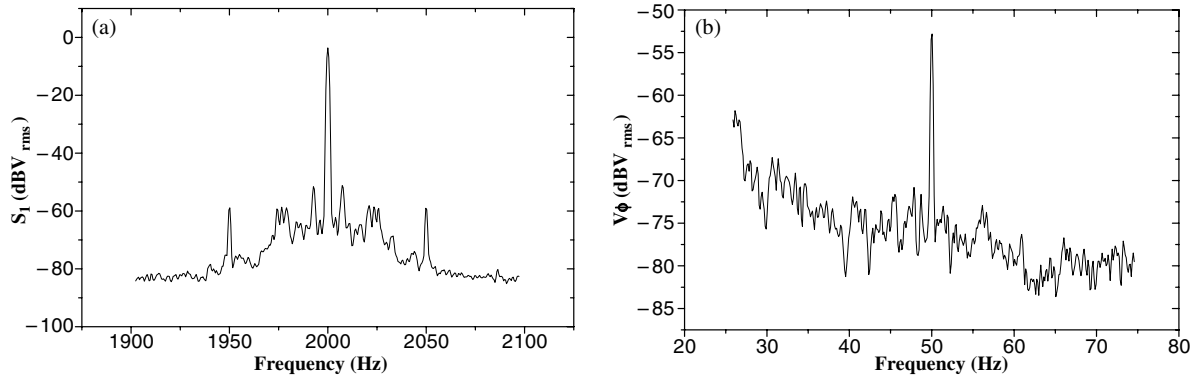

Figure 6. Spectra obtained with a current of 100 A_{rms} passing through the conductor: (*a*) carrier S_1; (*b*) phase ϕ_{S_1}.

A signal to noise ratio of 24.4 dB was measured in the phase spectrum, which corresponds to a resolution of 17 A_{rms} $Hz^{-1/2}$. Another way to determine the resolution is by real time monitoring of the RMS amplitude of the output phase waveform when the RMS amplitude of the current waveform in the conductor is stepped by a certain value. This procedure is illustrated in figure 7 for a RMS current step of 108 A_{rms}. The analysis of data in this figure indicates a resolution of ≈22.4 A_{rms} $Hz^{-1/2}$ (considering the detection bandwidth of 122 mHz), a value that is close to the one obtained with the alternative spectral approach. It is believed that this relatively modest resolution results from the high level of phase noise [10] present in the system. In fact, it was found that for the particular laser diode utilized in the experiment the modulation of the injection current induced significant spectral instability. This instability was then translated into the intensity noise via the optical path imbalance (≈6 cm) of the Mach–Zehnder interferometer. This means that, in principle, a significant improvement in the system resolution would be achieved if the wavelength of the laser was stabilized.

In the double reflection approach, the optical loop only performs Ampère's circuit law exactly if care is taken to work in almost ideal conditions [11]. No strong external magnetic fields can be present, and the conductor must be placed in the exact geometrical centre of the Sagnac loop in a position orthogonal to the sensing head plane. Although these precautions were taken into account during this experiment, in a practical situation any deviation from these conditions may degrade system performance.

In the experimental set-up, care was taken in deploying the optical fibre cables in order to minimize the vibration-induced noise associated with the micro-bending losses in multimode optical fibres. In a practical system, specific signal processing must be utilized to achieve the minimization of this problem [7].

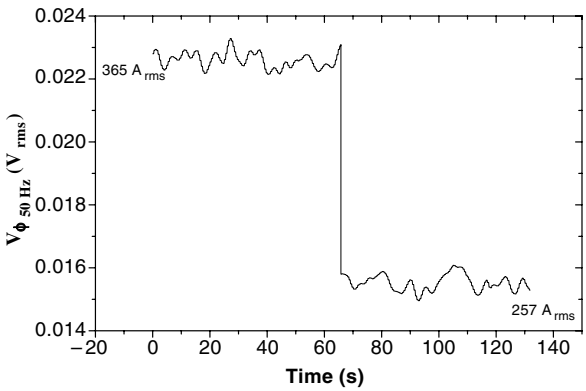

Figure 7. Amplitude (RMS) of the output phase signal at 50 Hz when a current step of 108 A_{rms} is applied.

The consideration of serrodyne processing limits measurement bandwidth to a value that should not exceed one tenth of the carrier frequency. This feature restricts the application of the proposed system to electric current metering applications and makes it unsuitable for relaying applications, i.e. for the monitoring of current line transients. However, this is not an intrinsic limitation of the sensor design shown in figure 1. Indeed, active homodyne processing could be implemented by using S_1 to feed a feedback loop that would act on the laser diode injection current in order to

keep the interferometer system at a fixed point of its transfer function (typically in quadrature). With such processing the information about the electrical current flowing along the conductor would be obtained from the value of the laser diode injection current. The measurement range and bandwidth would, therefore, only depend on the wavelength tunability of the laser diode radiation and on the bandwidth of the feedback loop, respectively.

5. Conclusion

Theoretical and experimental results were presented which validated a new dual interferometric configuration with serrodyne processing for the remote sensing of electrical current. Linearity and waveform reproduction at 50 Hz were observed and a current resolution $\approx 20\ A_{rms}\ Hz^{-1/2}$ was obtained. The utilization of the proposed interferometric concept to simultaneously perform metering and relaying current measurements was also addressed.

References

[1] Ning Y N, Wang Z P, Palmer A W and Gratan K T V 1995 Recent progress in optical current sensing techniques *Rev. Sci. Instrum.* **5** 3097–111

[2] Meggit B T and Grattan K T V 1999 *Optical Fiber Sensor Technology: Applications and Systems* (Dordrecht: Kluwer)

[3] Forman P R and Jahoda F C 1988 Linear birefringence effects on fiber-optic current sensors *Appl. Opt.* **27** 3088–96

[4] Chu B C B, Ning Y N and Jackson D A 1992 Faraday current sensor that uses a triangular-shaped bulk-optic sensing element *Opt. Lett.* **17** 1167–9

[5] Tadashi Sato, Genji Takahashi and Inui Y 1986 Method and apparatus for optically measuring a current *US Patent* n. 4564754 Hitachi, LTD

[6] Ning Y N, Chu B C B and Jackson D A 1991 Miniature Faraday current sensor based on multiple critical angle reflections in a bulk-optic ring *Opt. Lett.* **16** 1996–8

[7] Fisher N E and Jackson D A 1996 A common-mode optical noise-rejection scheme for an extrinsic Faraday current sensor *Meas. Sci. Technol.* **7** 796–800

[8] Yu A and Siddiqui A S 1993 A theoretical and experimental investigation of a practicable fibre optic current sensor using a Sagnac interferometer *Proc. OFS 9 (Florence, Italy)* (AEI, IROE-CNR) pp 289–92

[9] Pistoni N C 1995 Simplified approach to the Jones Calculus in retracing optical circuits *Appl. Opt.* **34** 7870–6

[10] Dandridge A and Tveten A B 1981 Phase noise of single-mode diode lasers in interferometer systems *Appl. Phys. Lett.* **39** 530–2

[11] Zheng Ping Wang, Wei Min Sun, Zong Jun Huang, Chong Kang, Sun Ling Ruan, Yao Hua Luo, Palmer A W and Grattan K T V 1998 Effects of reflection-induced retardance on the immunity of bulk optic-material current sensors *Appl. Opt.* **37** 7293–7